ALICE 3 and the quest for new physics phenomena at low transverse momentum

- ALICE, status and prospects for the coming decade
- the statistical hadronization model and (u,d,s) hadrons
- the Dashen-Ma-Bernstein S-matrix approach
- including loosely bound hadrons, light nuclei and hyper-nuclei
- from pp to Pb-Pb collisions
- outlook

pbm

42nd Erice International School of Nuclear Physics

Sep. 16-22, 2021

the Quark-Gluon Plasma formed in nuclear collisions at very high energy

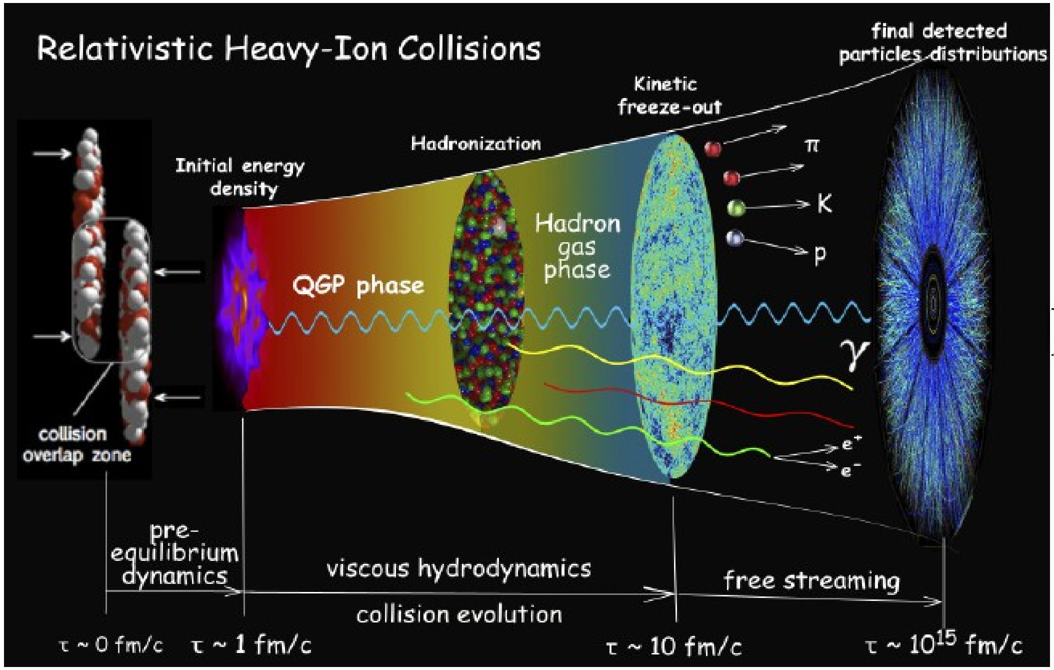

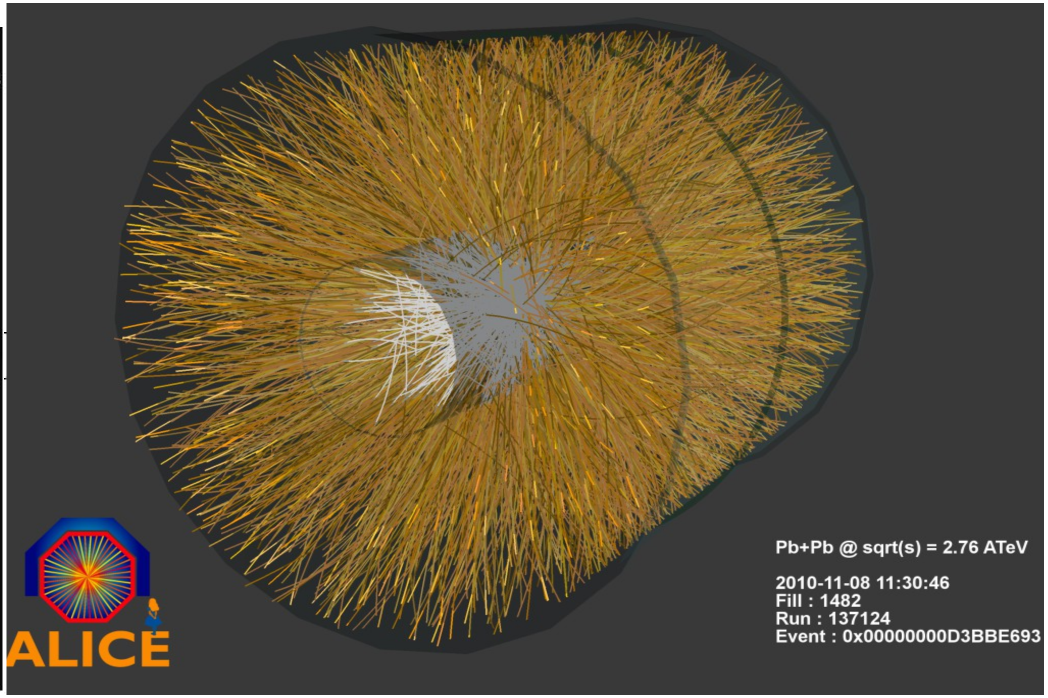

Paul Sorensen and Chun Shen

PbPb collisions at LHC at √s = 5.02 A TeV

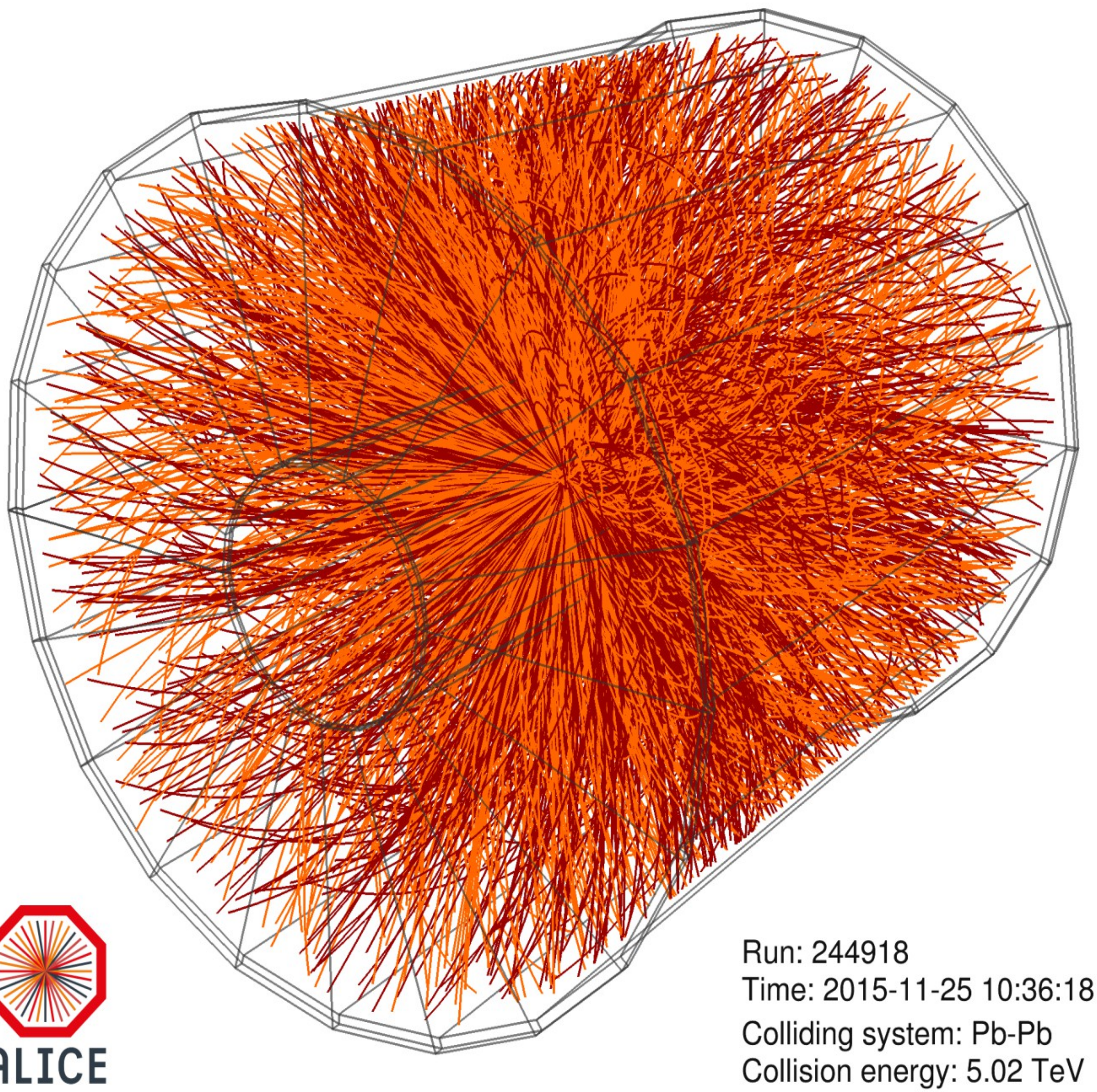

Run1: 3 data taking campaigns
pp, pPb, Pb—Pb
> 170 publications

Run2 with 13 TeV pp
Pb—Pb run 5 TeV/u
p-Pb Run at 5 and 8 TeV
> 50 publications

Nov. 2018: PbPb 5 TeV/u

Snapshot taken with the ALICE TPC

Nov. 2019: Run1 and Run2 combined: > 260 publications

central Pb-Pb collisions:
more than 32000
particles produced per collision
at top LHC energy

ALICE plans for the coming decade 2022 – 2030
LHC Run3 and Run4

ALICE is currently being upgraded:

GEM based read-out chambers for the TPC, new inner tracker with ultra-thin Si layers, continuous read of (all) subdetectors

increase of data rates by factor >50

focus on rare objects, exotic quarkonia, single (and possibly double) charm hadrons to address a number of fundamental questions and issues such as:

- what is the deconfinement radius for charm quarks
- are there colorless bound states in a deconfined medium?
- are complex, light nuclei and exotic charmonia (X,Y,Z) produced as compact multi-quark bags?
- can fluctuation measurements shed light on the mechanism of baryon production and critical behavior near the phase boundary?

- low mass dileptons and low-p_T thermal photons
- collectivity from pp to AA collisions
- nuclear and hadronic physics
  - structure of light hyper-nuclei
  - hadron-hadron interaction from particle correlations
- ultra-peripheral and diffractive collisions

deciphering QCD in the strongly coupled regime

ALICE plans for Run 3 and 4

Long-term LHC schedule

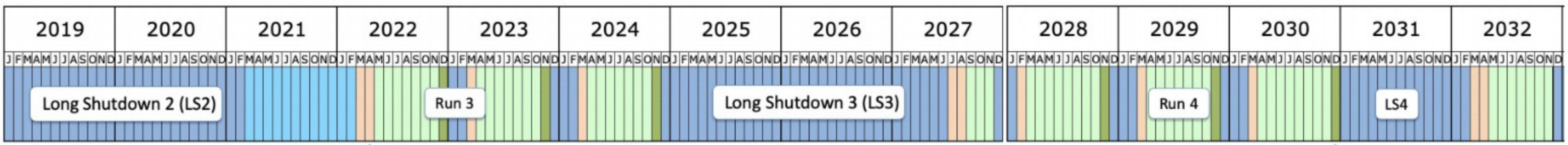

Run 1 + Run 2

$\mathcal{L}_{int}(Pb-Pb) \approx 1nb^{-1}$

$\mathcal{L}_{int}(Pb-Pb) \approx 13\, nb^{-1}$

Run 3 luminosity targets

Pb-Pb (**13 nb^{-1}**): x 10 increase wrt Run 1 + Run2 (max interaction rate 50 kHz)

⇨ ALICE continous detector readout (no trigger) and recording

⇨ **x 50 increase in statistics** for most observables (minimum-bias rate limited to 1 kHz in Runs 1 and 2)

not only Pb-Pb, but also pp (**200/pb**), p-Pb (**~0.6/pb**) and O-O (**~1/nb**)

main advantage of ALICE: particle identification with the ALICE TPC is preserved

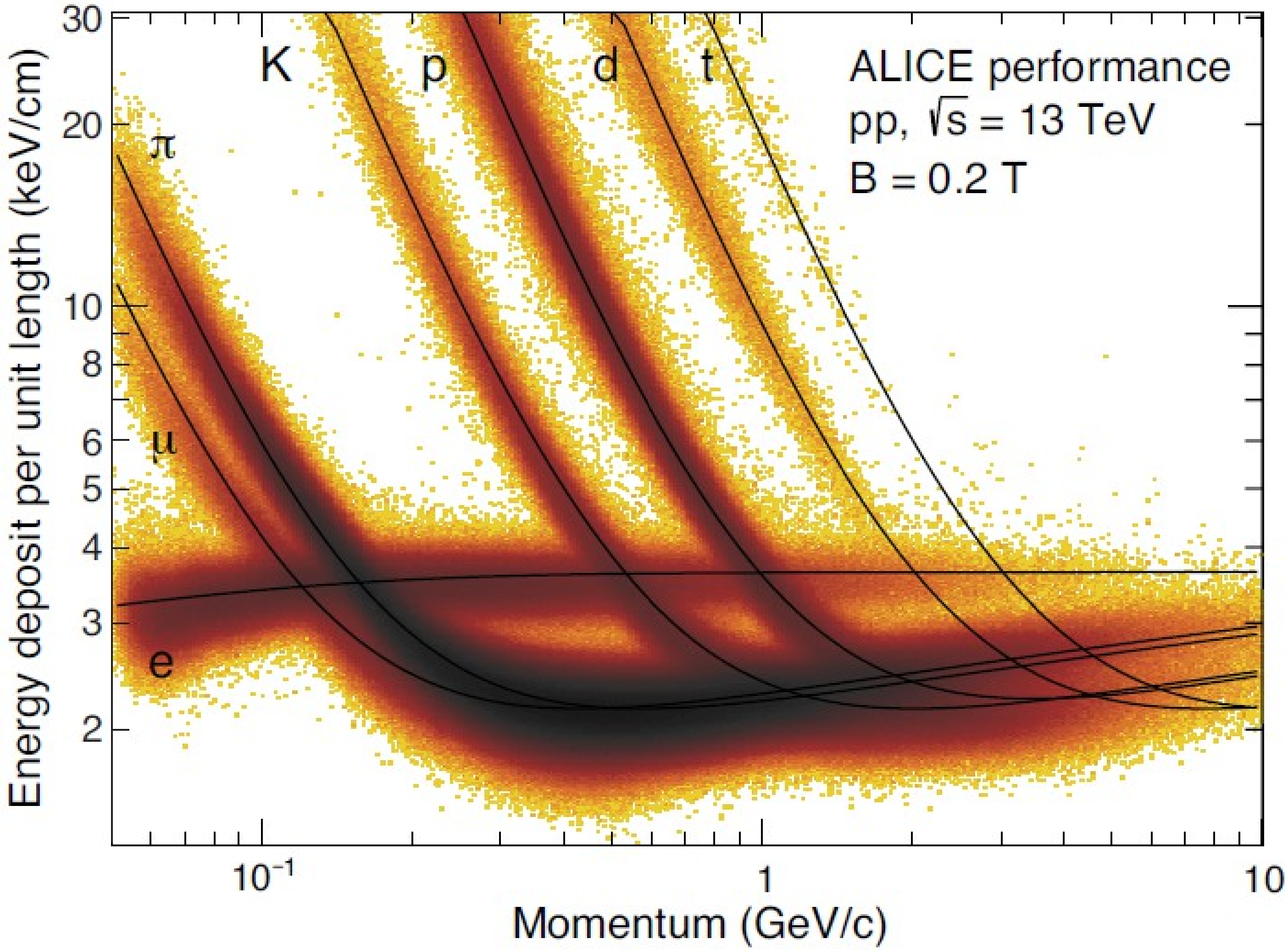

now PDG standard

M. Tanabashi et al. (Particle Data Group), Phys. Rev. D 98, 030001, Fig. 34.15

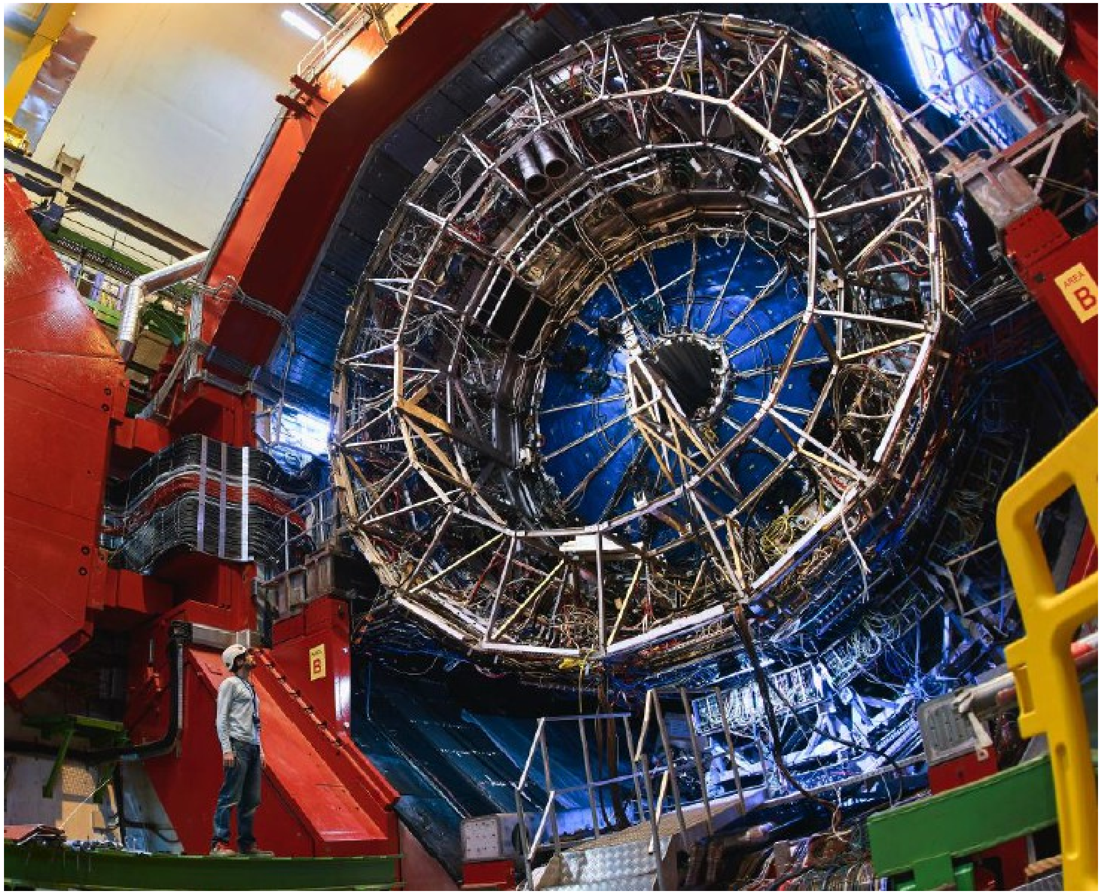

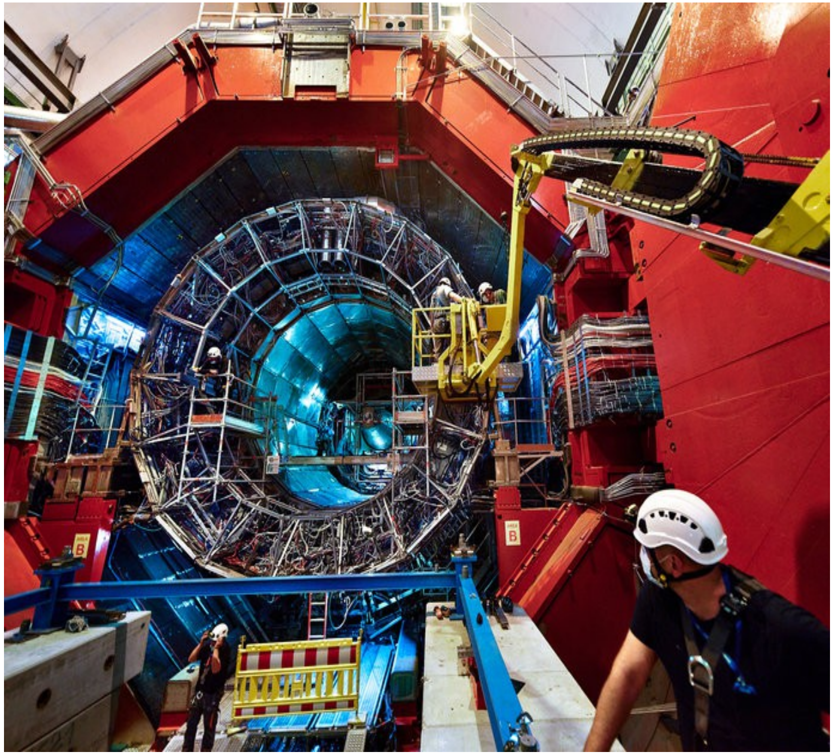

installation of upgraded detectors
TPC and (new) ITS
March 25, 2021

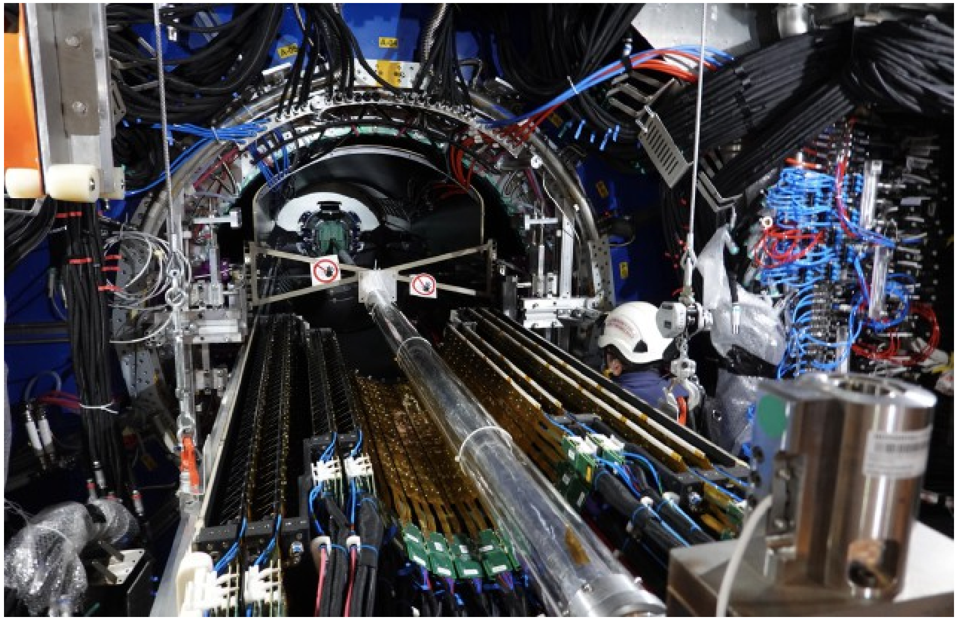

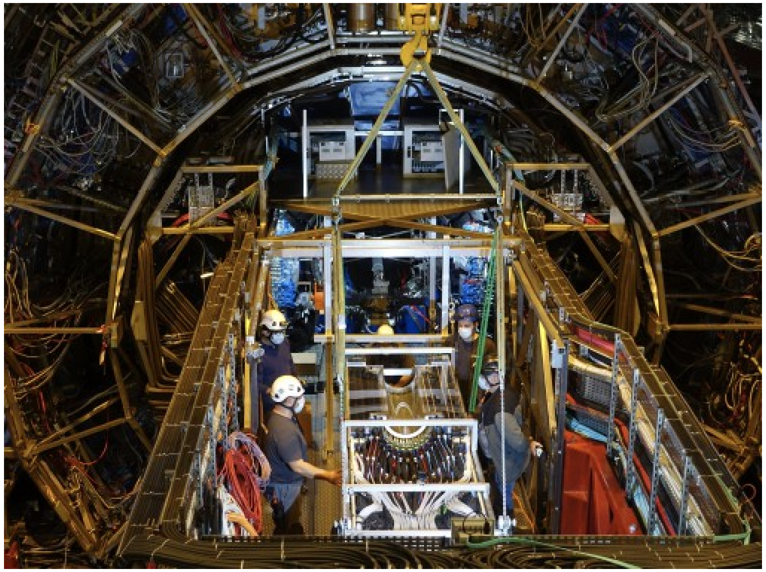

hadron production and the QCD phase boundary

measure the momenta and identity of all produced particles at all energies and look for signs of equilibration, phase transitions, regularities, etc

at the phase boundary, all quarks and gluons are converted ('hadronized') into hadrons which we measure in our detectors

main aim: establish the existence and position of the phase boundary

an important milestone also for understanding the evolution of the early universe

statistical hadronization model of particle production

partition function Z(T,V) contains sum over the full hadronic mass spectrum and is fully calculable in QCD

for each particle i, the statistical operator is:

$$\ln Z_i = \frac{V g_i}{2\pi^2} \int_0^\infty \pm p^2 \mathrm{d}p \ln[1 \pm \exp(-(E_i - \mu_i)/T)]$$

particle densities are then calculated according to:

$$n_i = N_i/V = -\frac{T}{V}\frac{\partial \ln Z_i}{\partial \mu} = \frac{g_i}{2\pi^2} \int_0^\infty \frac{p^2 \mathrm{d}p}{\exp[(E_i - \mu_i)/T] \pm 1}$$

from analysis of all available nuclear collision data we now know the energy dependence of the parameters T, mu_b, and V over an energy range from threshold to LHC energy and can confidently extrapolate to even higher energies

in practice, we use the full experimental hadronic mass spectrum from the PDG compilation (vacuum masses) to compute the 'primordial yield'

comparison with measured hadron yields needs evaluation of all strong decays

statistical hadronization of (u,d,s) hadrons

A. Andronic, P. Braun-Munzinger, K. Redlich, J. Stachel, Nature 561 (2018) 321

status as of Sep. 2021

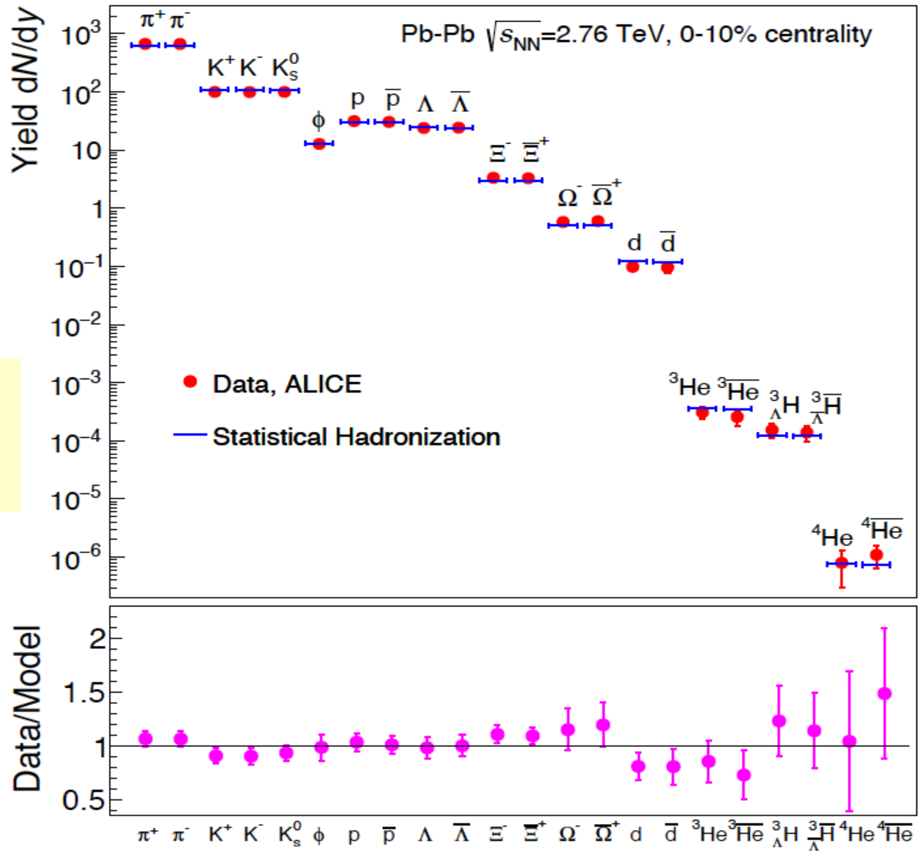

Best fit:

$T_{CF} = 156.6 \pm 1.7$ MeV

$\mu_B = 0.7 \pm 3.8$ MeV

$V_{\Delta y=1} = 4175 \pm 380$ fm^3

$\chi^2/N_{df} = 16.7/19$

S-matrix treatment of interactions (non-strange sect.)

"proton puzzle" solved

PLB 792 (2019) 304

data: ALICE coll., Nucl. Phys. A971 (2018) 1

agreement over 9 orders of magnitude with QCD statistical operator prediction
(- strong decays need to be added)

- matter and antimatter formed in equal portions
- even large very fragile (hyper) nuclei follow the systematics

similar results at lower energy, each new energy yields a pair of (T, μ_B) values

connection to QCD (QGP) phase diagram

the proton anomaly and the Dashen, Ma, Bernstein S-matrix approach

R. Dashen, S. K. Ma, and H. J. Bernstein, Phys. Rev. **187**, 345 (1969).

The S-matrix formalism [20–24] is a systematic framework for incorporating interactions into the description of the thermal properties of a dilute medium. In this scheme, two-body interactions are, via the scattering phase shifts, included in the leading term of the S-matrix expansion of the grand canonical potential. The resulting interacting density of states is then folded into an integral over thermodynamic distribution functions, which, in turn, yields the interaction contribution to a particular thermodynamic observable.

thermal yield of an (interacting) resonance with mass M, spin J, and isospin I

$$\langle R_{I,J}\rangle = d_J \int_{m_{th}}^{\infty} dM \int \frac{d^3p}{(2\pi)^3}\,\frac{1}{2\pi}\,B_{I,J}(M) \times \frac{1}{e^{(\sqrt{p^2+M^2}-\mu)/T}+1},$$

A. Andronic, pbm, B. Friman, P.M. Lo, K. Redlich, J. Stachel, arXiv:1808.03102, Phys.Lett.B792 (2019)304

need to know derivatives of phase shifts with respect to invariant mass

$$B_{I,J}(M) = 2\,\frac{d\delta_J^I}{dM}.$$

pion nucleon phase shifts and thermal weights for N* and Δ resonances

GWU/SAID phase shift analysis, 15 partial waves for each isospin channel

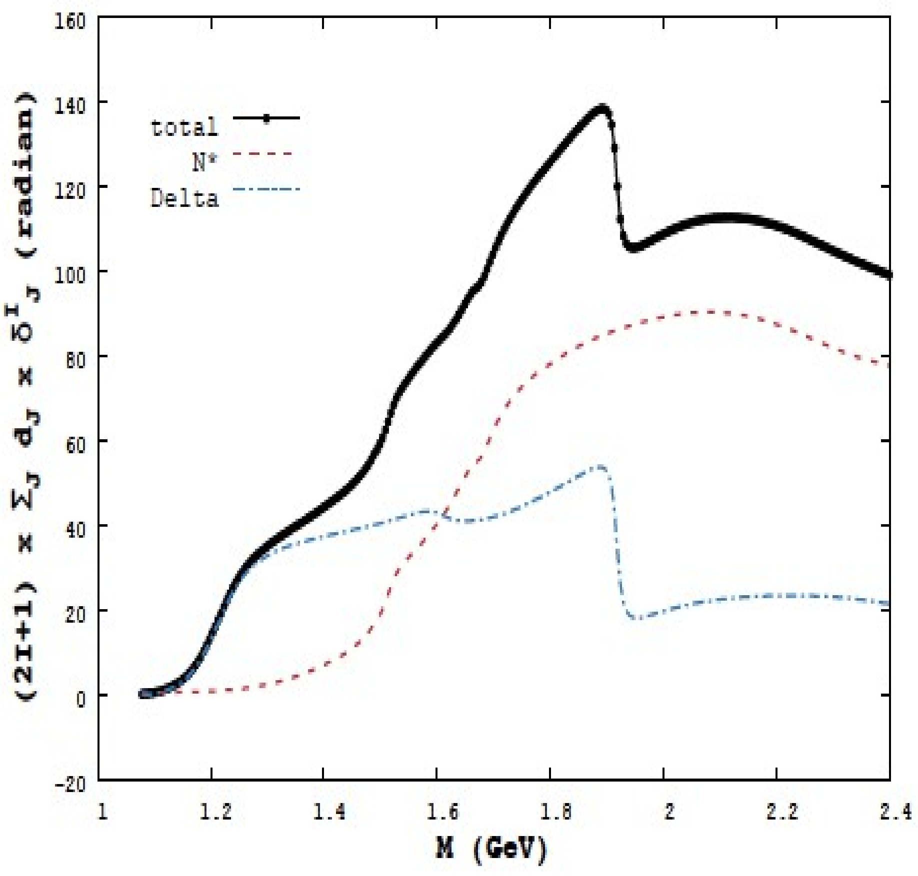

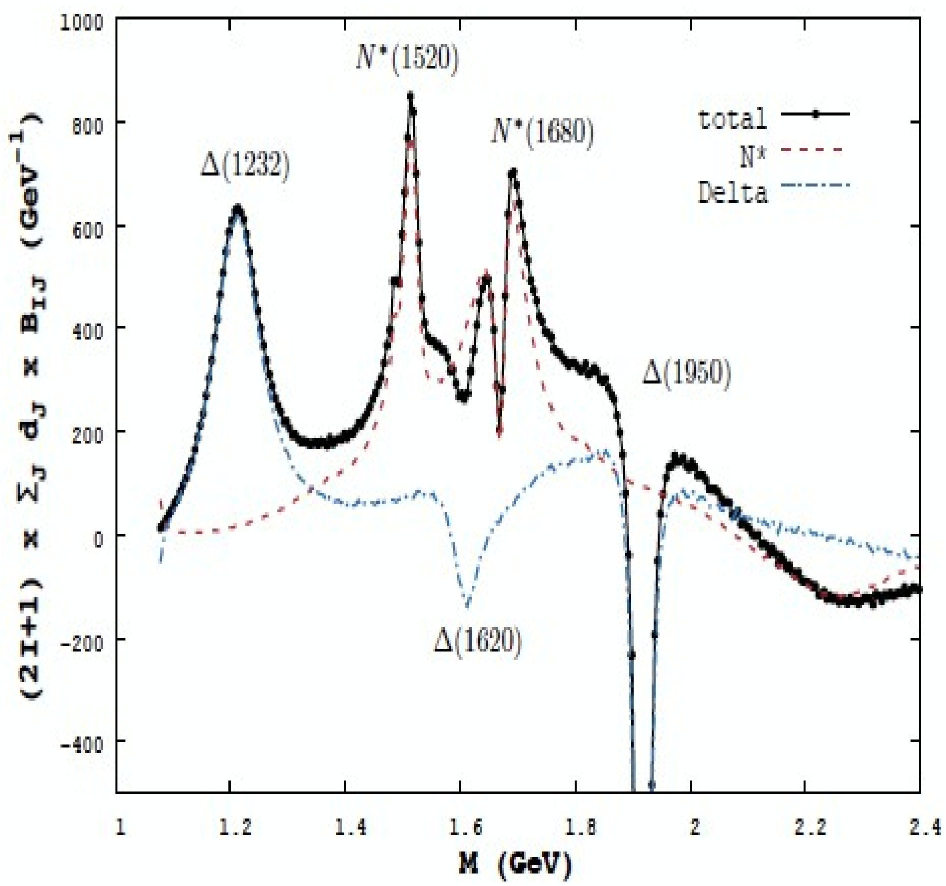

at LHC energy, production of (u,d,s) hadrons is governed
by mass and quantum numbers only
quark content does not matter

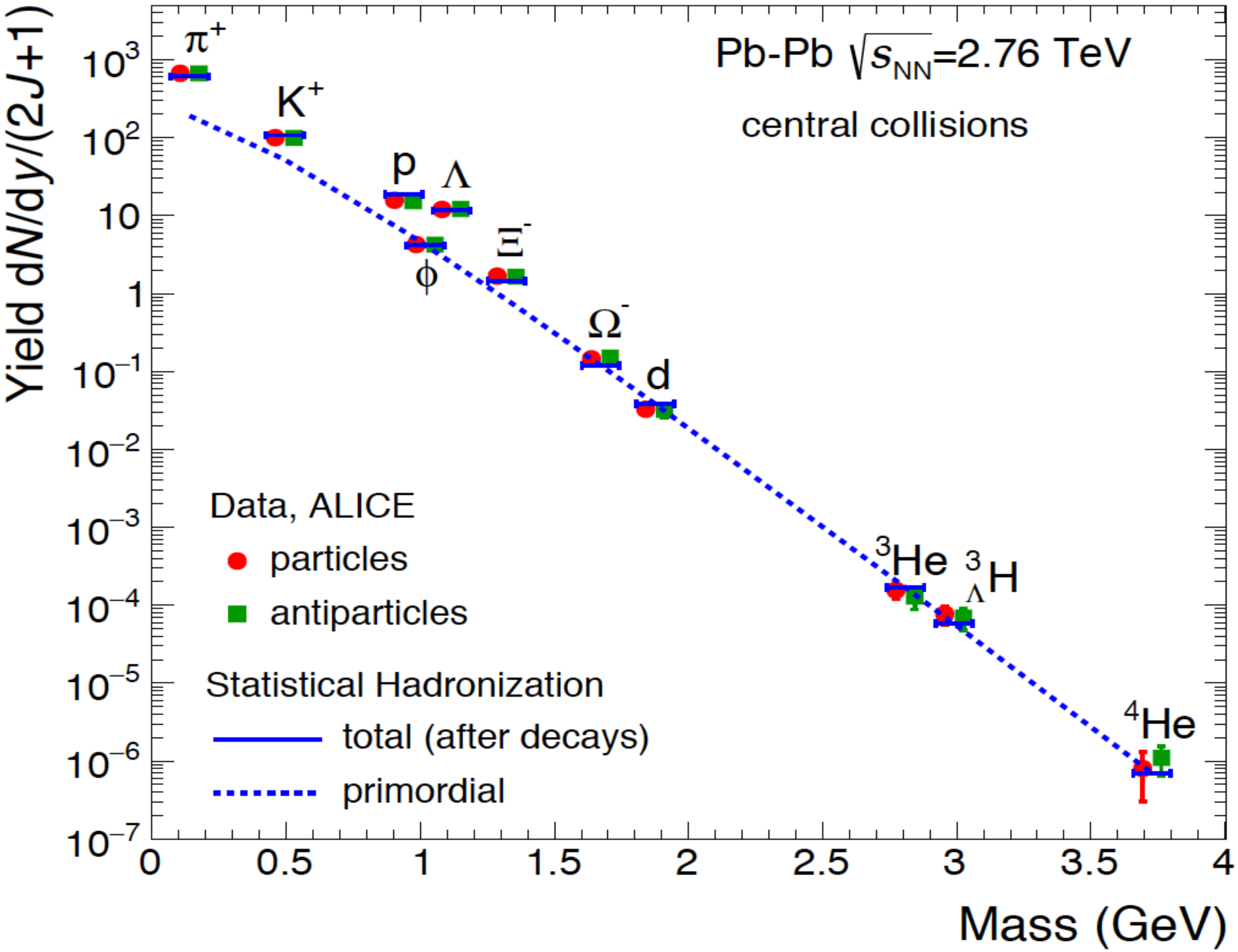

universal hadronization

1 parameter (T)

at LHC energy, matter and anti-matter is
produced with equal yields

energy dependence of hadron production described quantitatively

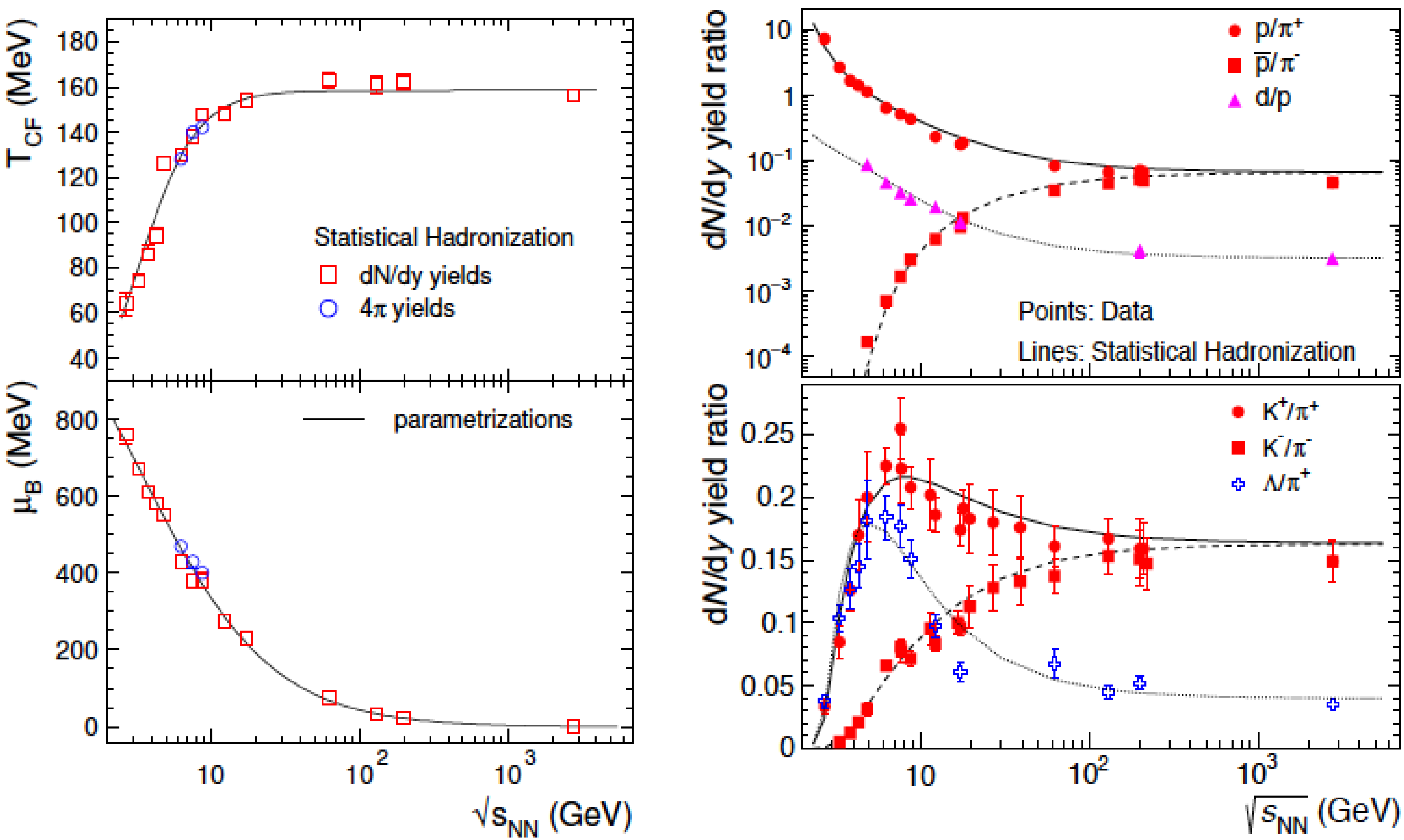

together with known energy dependence of charged hadron production in Pb-Pb collisions we can predict yield of all hadrons at all energies with < 10% accuracy

the QGP phase diagram, LatticeQCD, and hadron production data

note: all coll. at SIS, AGS, SPS, RHIC and LHC involved in data taking
each entry is result of several years of experiments, variation of μ_B via variation of cm energy

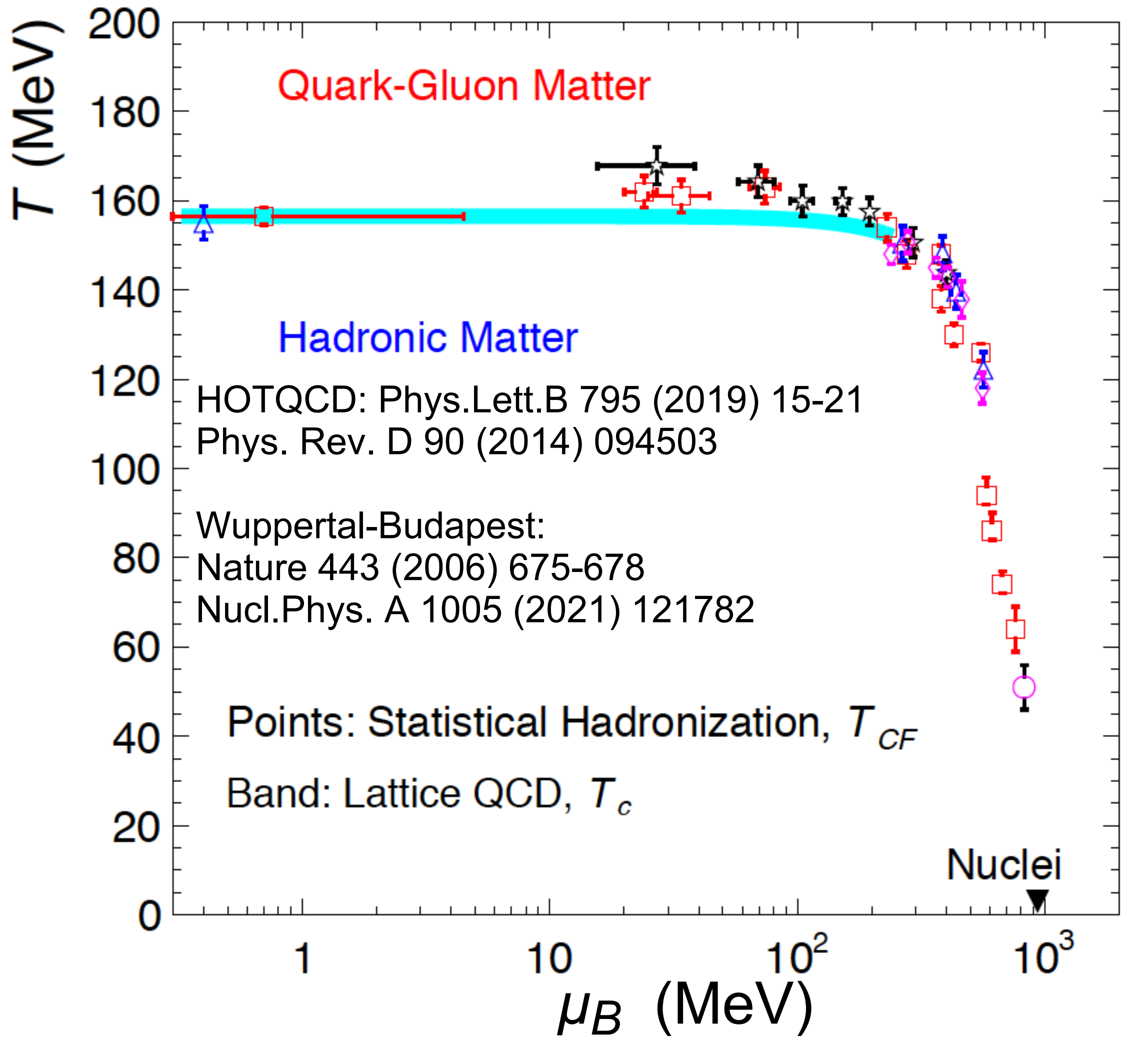

quantitative agreement of chemical freeze-out parameters with most recent LQCD predictions for baryo-chemical potential < 300 MeV

cross over transition at μ_B = 0 MeV, no experimental confirmation

should the transition be 1st order for large μ_B (large net baryon density)?

then there must be a critical endpoint in the phase diagram

experimental determination of phase boundary at
T_c = 156.6 ± 1.7 (stat.) ± 3 (syst.) MeV and μ_B = 0 MeV
Nature 561 (2018) 321

now on very loosely bound states and their production in high energy collisions

- already the deuteron with 2.2 MeV binding enery is very loosely bound compared to the average energy of particles at the LHC (TeV)
- the hyper-triton is an even more extreme case, see below
- the quantum mechanical formation time of such states far exceeds 100 fm/c, i.e. they cannot be generated or destroyed more than once in a collision

The Hypertriton

mass = 2990 MeV, binding energy = 2.3 MeV

Lambda sep. energy = 0.13 MeV

molecular structure: (p+n) + Lambda

2-body threshold: (p+p+n) + pi- = ^{3}He + pi-

rms radius = $(4\ \mathrm{B.E.}\ M_{red})^{-1/2}$ = 10.3 fm =
rms separation between d and Lambda

in that sense: hypertriton = (p n Lambda) =
(d Lambda) is the ultimate halo state

yet production yield is fixed at 156 MeV temperature
(about 1000 x Lambda separation energy.)

wave function of the hyper-triton – schematic picture

figure by Benjamin Doenigus, August 2017

triton

hyper-triton

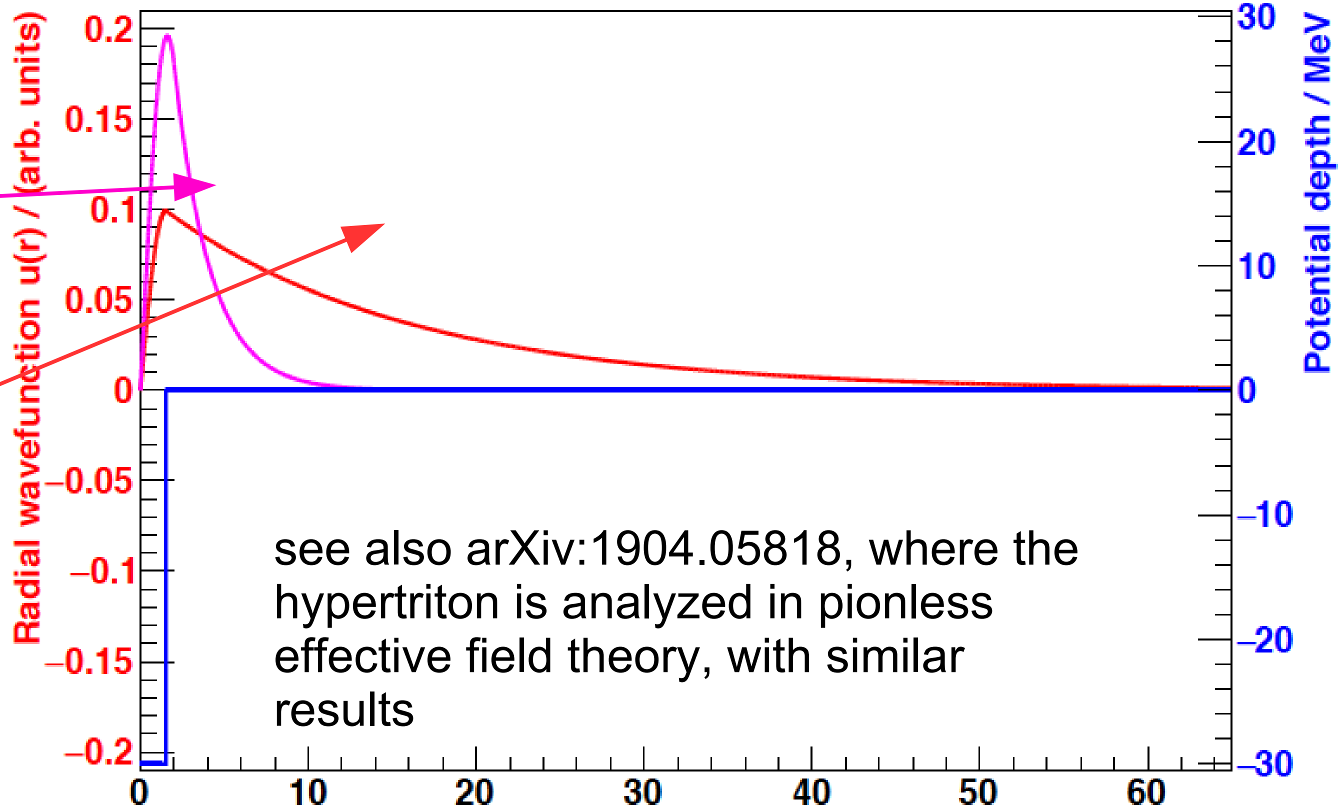

Wavefunction (red) of the hypertriton assuming a s-wave interaction for the bound state of a Λ and a deuteron. The root mean square value of the radius of this function is $\sqrt{\langle r^2 \rangle} = 10.6$ fm. In blue the corresponding square well potential is shown. In addition, the magenta curve shows a "triton" like object using a similar calculation as the hypertriton, namely a deuteron and an added nucleon, resulting in a much narrower object as the hypertriton.

now most recent results on hyper-triton structure from ALICE precision measurements

- binding energy
- Λ separation energy
- lifetime

Lifetime & yield of hypernuclei

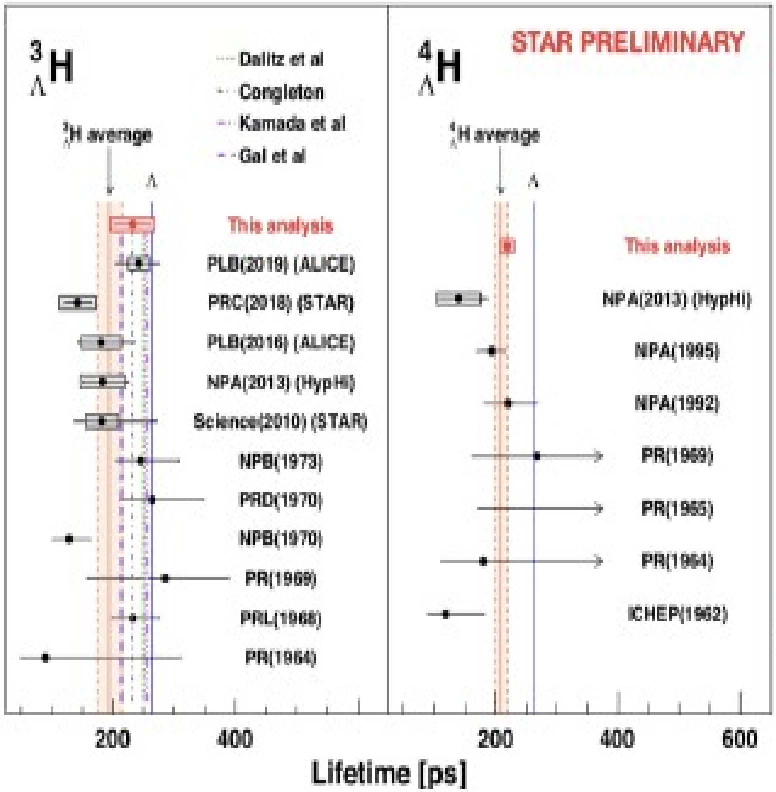

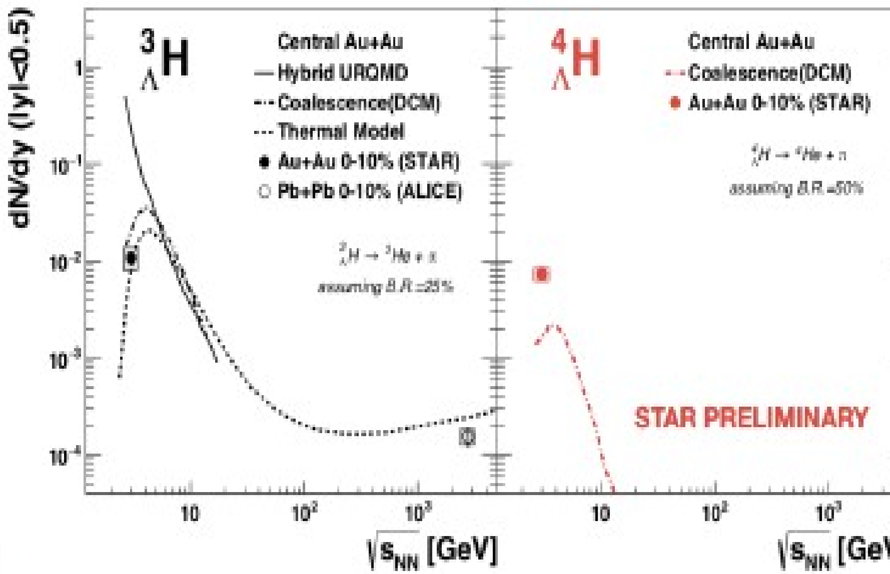

hyper-triton identification in ALICE using machine-learning techniques

BDT

for boosting the signal extraction

- Boosted Decision Trees (BDT) models trained on dedicated sample to discriminate signal and background
- State-of-the-art hyperparameter optimization
- BDT selection optimized to improve the significance of the hypertriton signal
- Signal extracted with high significance over a wide ct range

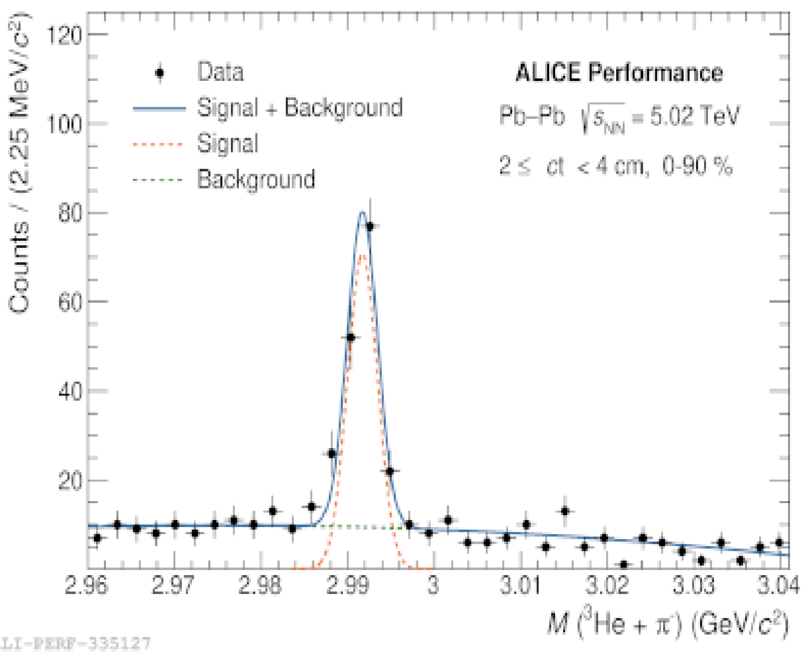

very small background contribution

newest result on lifetime measurement – needs precision determination of ALICE detector material

Lifetime

measurement

- Signal extracted in a wide ct range thanks to the BDT
- Most precise hypertriton lifetime determination so far
  - 5% stat. 6% syst.
  - Statistical uncertainty lower than the world average uncertainty
- Consistent with free Λ lifetime and previous ALICE measurement

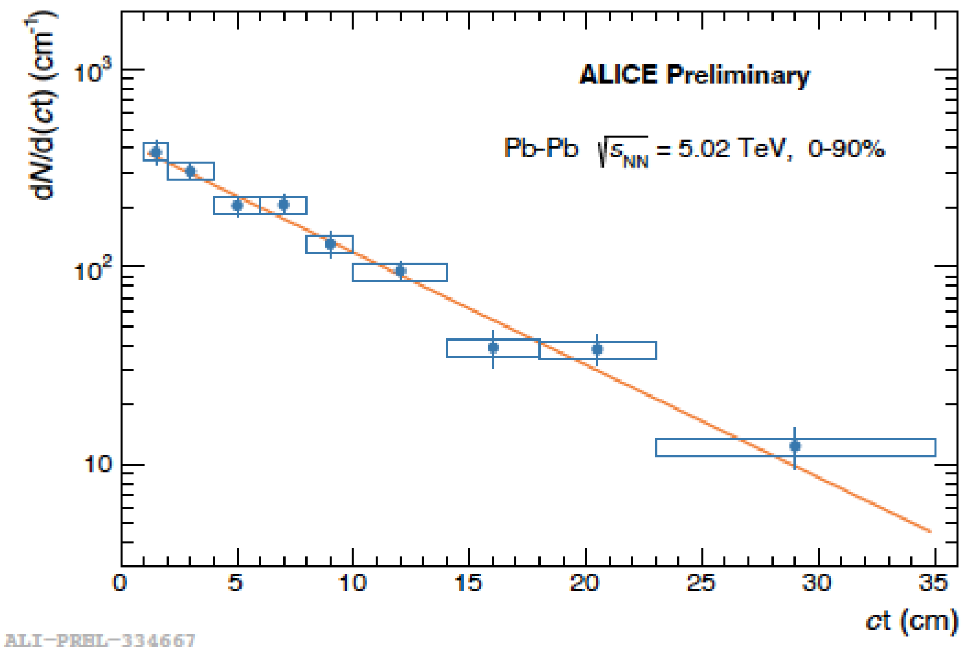

newest ALICE results strongly support loosely bound structure of hyper-triton

Lifetime
measurement

- Signal extracted in a wide ct range thanks to the BDT
- Most precise hypertriton lifetime determination so far
  - 5% stat. 6% syst.
  - Statistical uncertainty lower than the world average uncertainty
- Consistent with free Λ lifetime and previous ALICE measurement

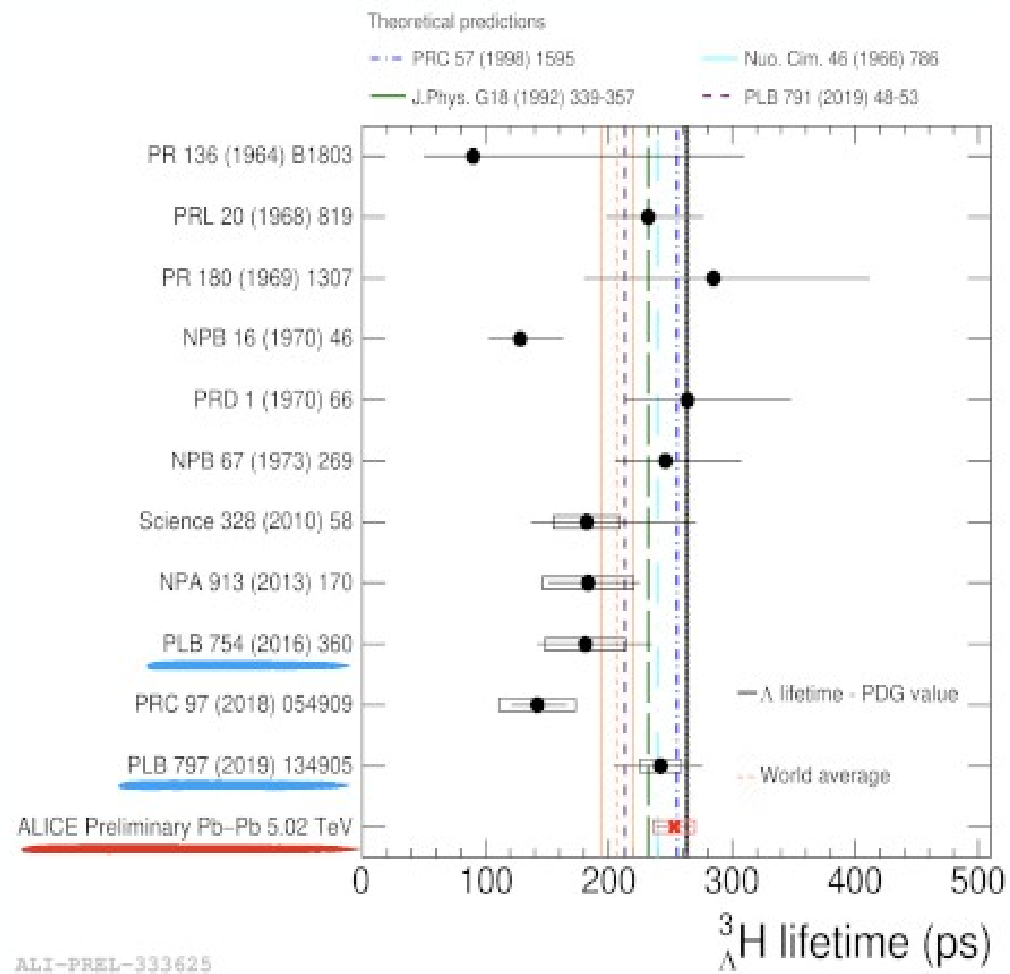

new ALICE results on hyper-triton binding energy

- Use Machine Learning (BDTs) to identify ${}^{3}_{\Lambda}\mathrm{H}$ candidates in Pb–Pb
- Most precise measurement of ${}^{3}_{\Lambda}\mathrm{H}$ lifetime
  - Favors ${}^{3}_{\Lambda}\mathrm{H}$ lifetime near free Λ lifetime
- Very precise measurements of ${}^{3}_{\Lambda}\mathrm{H}$ mass and binding energy
  - Binding energy compatible with 0.
  - Support loosely bound ${}^{3}_{\Lambda}\mathrm{H}$

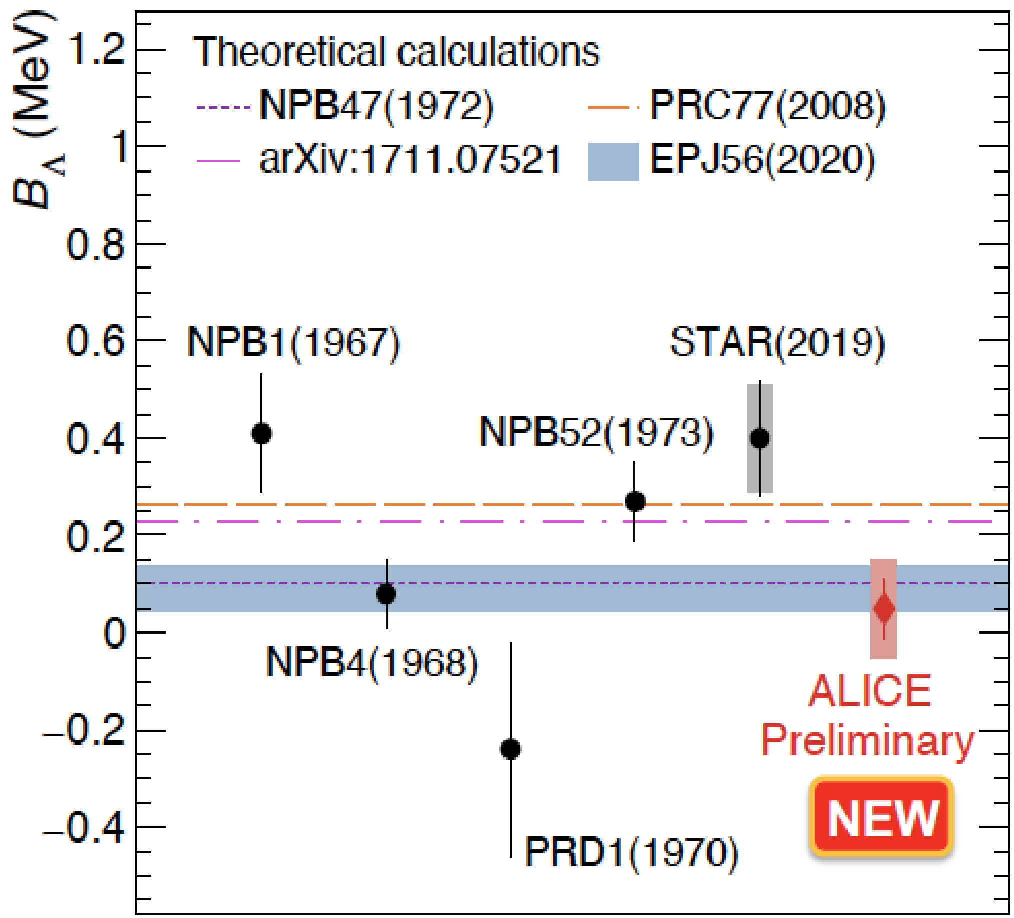

note: measurement of B_{Λ}: 100 keV precision out of 2.99 GeV mass, dm/m = 1/30000

some considerations on bound state formation in relativistic nuclear collisions

- in general, bound states have finite formation time t_F
- bound state formation is a quantum mechanical process
- $t_F = 1/E_B$ as guideline
- for deuteron production, E_B = 2.2 MeV and t_F = 90 fm >> collision time
- for hyper-triton, use 'molecular structure' d-Λ
  t_F = 1/0.13 MeV = 1500 fm
- sudden approximation as used in coalescence models inappropriate
- loosely bound state cannot be described in multiple collision models, see e.g. Oliinychenko et al.,
  Phys.Rev.C 103 (2021) 3, 034913, 2009.01915 [hep-ph]

extension of SHM description to production in light systems from Pb-Pb to pPb to pp

need canonical thermodynamics and extended S-matrix approach

'the S-matrix calculation is based on the empirical phase shifts of πN scattering, an estimate of the ππN background constrained by Lattice QCD results of baryon-charge susceptibility, and an existing coupled-channel model describing the |S| = 1 strange baryons. an accurate description results of the widths of resonances and the non-resonant interactions in the thermal model. this leads to a reduction of the proton yield relative to the HRG baseline (by ≈ 25%). including the protons from strong decays of |S| = 1 hyperons, which constitute ≈ 6% of the total yields, does not alter this conclusion. '

adapted from:

Cleymans, Lo, Redlich, Sharma, Phys.Rev.C 103 (2021) 1, 014904, 2009.04844 [hep-ph]

hyper-triton production from pp to Pb-Pb collisions coalescence vs statistical hadronization model

- First measurements of ${}^{3}_{\Lambda}\mathrm{H}$ yields in pp (high-multiplicity) & p–Pb
- Results: ${}^{3}_{\Lambda}\mathrm{H}/\Lambda$ yield ratio

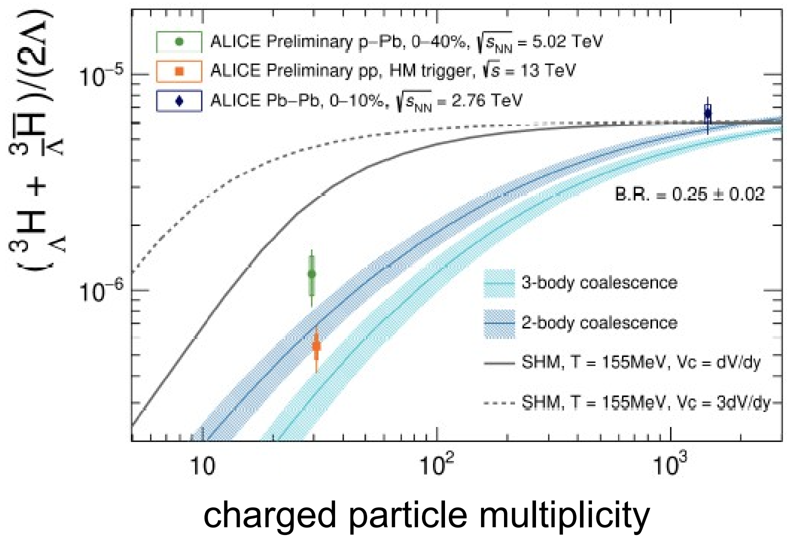

inconclusive: no S-matrix correction for protons

S-matrix correction for strange baryons

Cleymans, Lo, Redlich, Sharma, Phys.Rev.C 103 (2021) 1, 014904, 2009.04844 [hep-ph]

channel	elastic	channel	quasi-elastic	channel	unitarity
1	$\bar{K}N$	6	$\bar{K}_1^* N$	15	$\pi\pi\Lambda$
2	$\pi\Sigma$	7	$[\bar{K}_3^* N]_-$	16	$\pi\pi\Sigma$
3	$\pi\Lambda$	8	$[\bar{K}_3^* N]_+$		
4	$\eta\Lambda$	9	$[\pi\Sigma(1385)]_-$		
5	$\eta\Sigma$	10	$[\pi\Sigma(1385)]_+$		
		11	$[\bar{K}\Delta(1232)]_-$		
		12	$[\bar{K}\Delta(1232)]_+$		
		13	$[\pi\Lambda(1520)]_-$		
		14	$[\pi\Lambda(1520)]_+$		

TABLE I. The list of interaction channels included in the coupled-channel PWA describing the $|S| = 1$ hyperon system by the Joint Physics Analysis Center (JPAC) Collaboration [70]. Note that $\bar{K}^*$ is spin one and together with a nucleon can couple to spin 1/2 (denoted $\bar{K}_1^* N$) and spin 3/2 (denoted $\bar{K}_3^* N$). Subindices $\pm$ represent the higher and lower orbital angular momentum states which couple to a given partial wave.

no phase shift measurements available, use plane wave coupled channel approach instead

correlation volume dependence of canonical approach

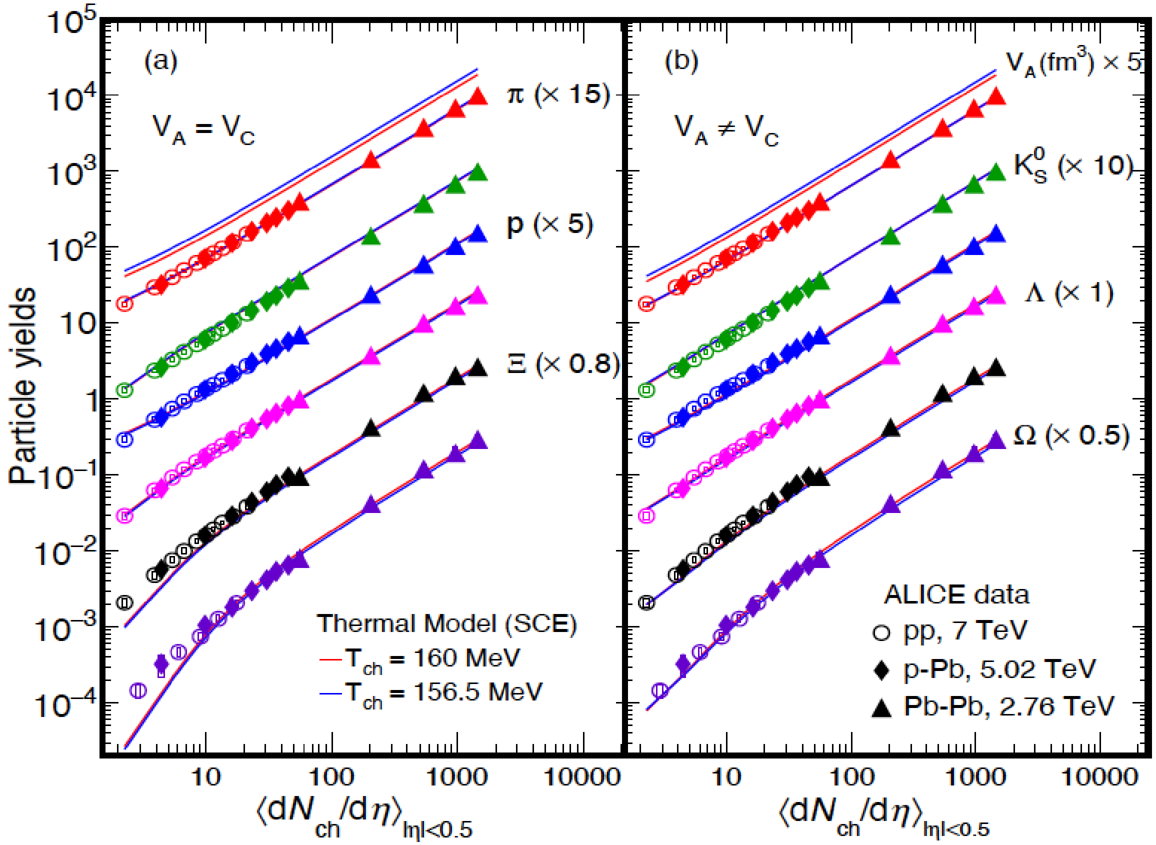

Cleymans, Lo, Redlich, Sharma, Phys.Rev.C 103 (2021) 1, 014904, 2009.04844 [hep-ph]

excellent description of ALICE data from Pb-Pb to pp collisions

ratio of yields to pions

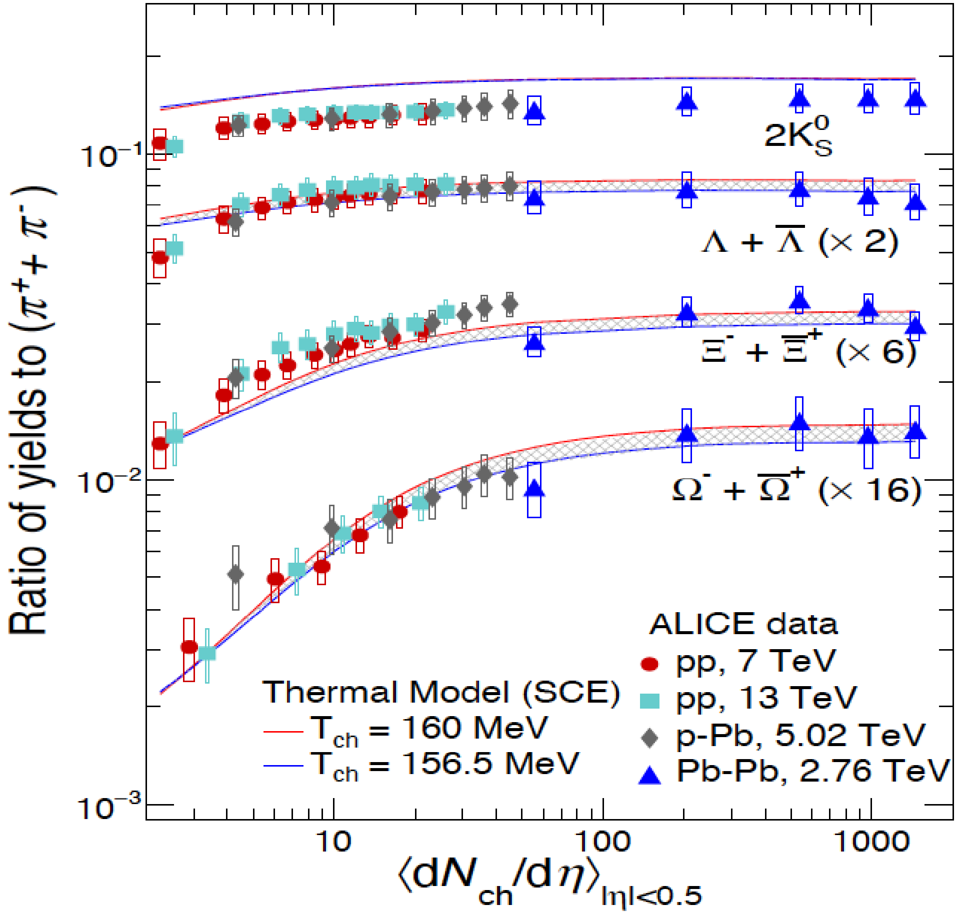

Cleymans, Lo, Redlich, Sharma, Phys.Rev.C 103 (2021) 1, 014904, 2009.04844 [hep-ph]

an unexpected surprize:
production yields and spectra of loosely bound and strongly bound objects simultaneously described in the SHMc

J/ψ and hyper-triton yields precisely described by Statistical Hadronization Model

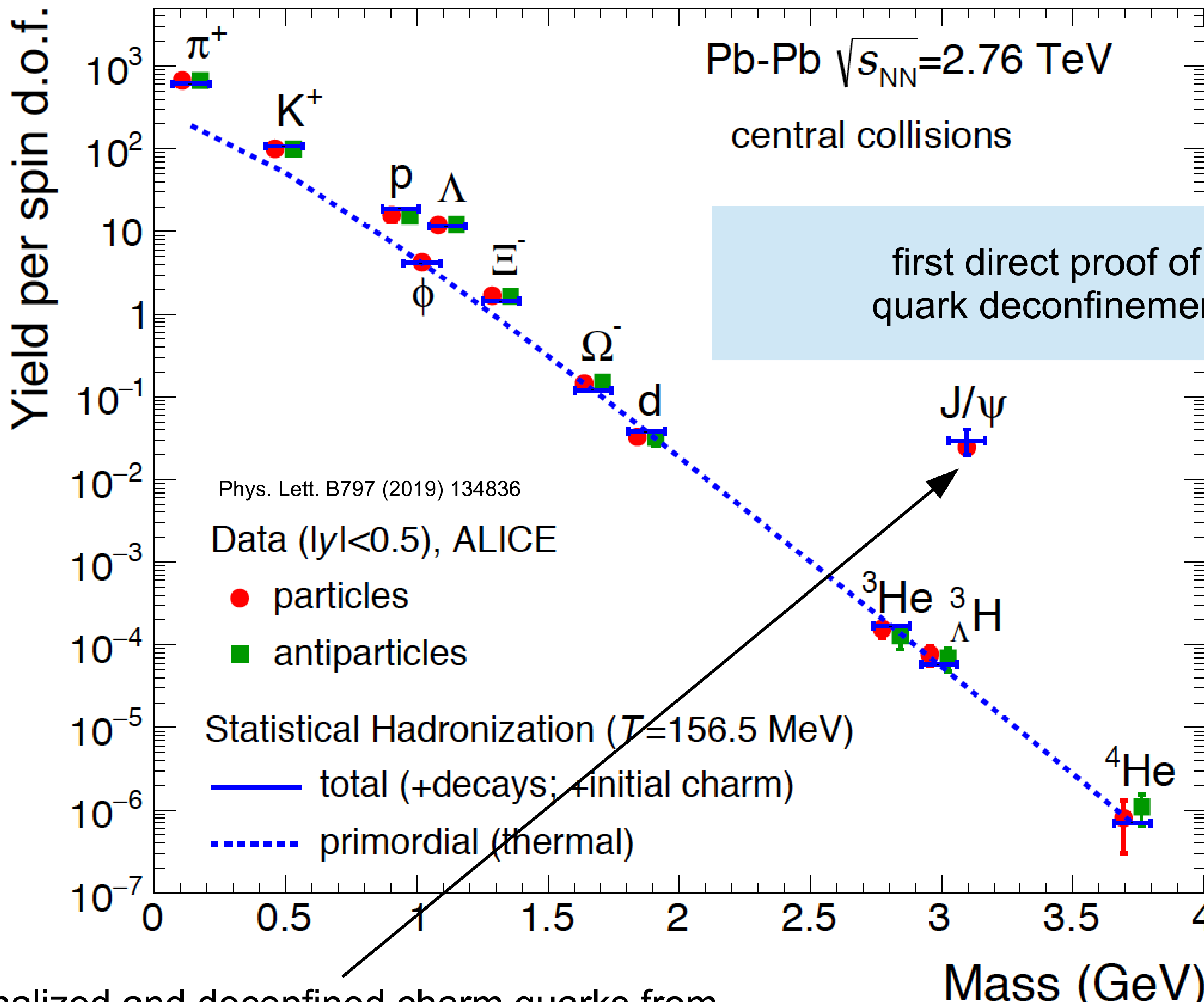

first direct proof of
quark deconfinement

with thermalized and deconfined charm quarks from
initial hard scattering

Andronic, pbm, Koehler, Redlich, Stachel,
Phys. Lett B797 (2019) 134836

J/ψ and hyper-triton yields described with the same flow parameters in the statistical hadronization model

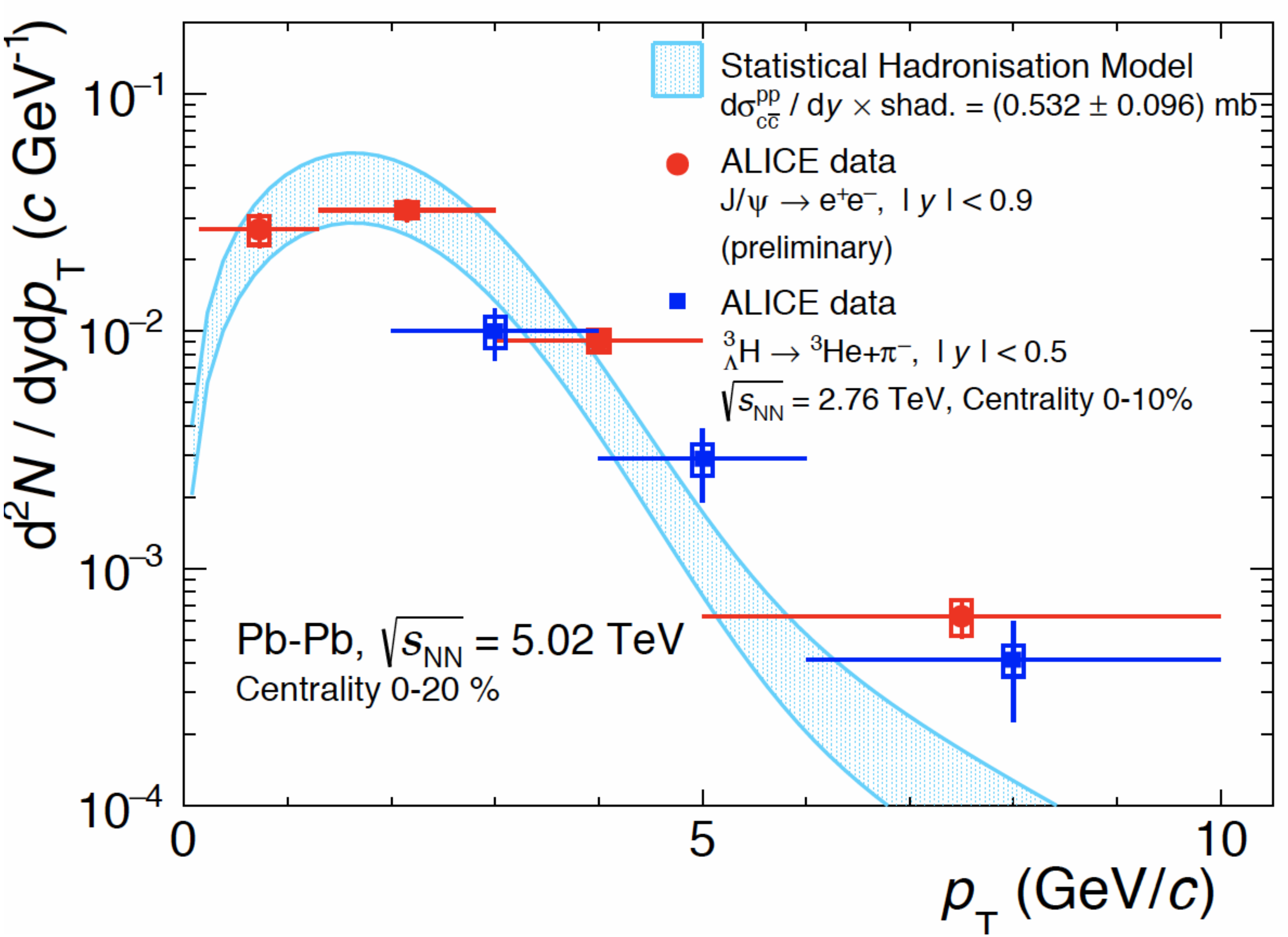

binding energies:
J/ψ   600 MeV
hypertriton   2.2 MeV
Lambda S.E. 0.13 MeV

from review: hypernuclei and other loosely bound objects produced in nuclear collisions at the LHC,
pbm and Benjamin Doenigus,
Nucl. Phys. A987 (2019) 144, arXiv:1809.04681

how are loosely bound states produced in high energy nuclear collisions?

doorway state hypothesis:
all nuclei and hyper-nuclei, penta-quark and T,X,Y,Z states are formed as virtual, compact multi-quark states at the phase boundary. Then slow time evolution into hadronic representation. Excitation energy about 20 MeV, time evolution about 10 fm/c

Andronic, pbm, Redlich, Stachel
Nature 561 (2018) 321, arXiv :1710.09425

how can this be tested?

precision measurement of spectra and flow pattern for light nuclei and hyper-nuclei, multi-charm hadrons, penta-quark and X,Y,Z states from pp via pPb to Pb-Pb

a major new opportunity for ALICE Run3/4 and beyond 2030 for X,Y,Z, T_{cc} and penta-quark states

also new opportunities for GSI/FAIR and JINR/NICA experiments